CONTROL AND SYNCHRONIZATION OF CHAOS
IN AN INDUCTION MOTOR SYSTEM

DIYI CHEN[1], PENG SHI[2,3] AND XIAOYI MA[1]

[1]Department of Electrical Engineering
Northwest A&F University
No. 3, Taicheng Road, Yangling 712100, P. R. China
diyichen@nwsuaf.edu.cn; ieee307@163.com

[2]Department of Computing and Mathematical Sciences
University of Glamorgan
Pontypridd, CF37 1DL, United Kingdom
peng.shi@vu.edu.au

[3]School of Engineering and Science
Victoria University
PO BOX 14428, Melbourne, VIC 8001, Australia

ABSTRACT. *This paper brings attention to the nonlinear dynamics of an induction motor's drive system with indirect field controlled. To understand the complex dynamics of system, some basic dynamical properties, such as equilibrium, stability are rigorously derived and studied. Chaotic attractors are first numerically verified through investigating phase trajectories, bifurcation path, Poincaré projections and dissipativity. Furthermore, a new sliding mode control method is proposed to gain the synchronization with different initial values. It can control the system to an equilibrium point. Numerical simulations are presented to demonstrate the effectiveness of the proposed controllers.*
Keywords: Induction motor, Chaos, Chaos control, Synchronization

1. **Introduction.** Chaotic behavior has been extensively analyzed in many fields such as mathematics [1], physics [2], biology [3], mechanical [4] and electrical engineering [5]. As a matter of fact, chaos may occur in natural processes. Controlling these complex chaotic dynamics for engineering applications has emerged as a new and attractive field and has developed many profound theories and methodologies.

Motor is a device, which is widely applied in industry for energy conversion between energy and mechanical energy. Many achievements have been proposed. For example, Ataei et al. [6] characterized the complex dynamics of the permanent-magnet synchronous motor (PMSM) model with a non-smooth-air-gap. A bifurcation analysis was applied to a Permanent Magnet (PM) stepper motor, and the nonlinear control was designed by Jing, Yu and Chen [7]. Harb and Zaher [8] studied chaotic behaviors in Permanent Magnet Synchronous Motor (PMSM) for a certain range of its parameters, and it was eliminated by using optimal Lyapunov exponent methodology. Zribi and his co-workers [9] proposed to use an instantaneous Lyapunov exponent control algorithm to control the Permanent Magnet Synchronous Motor (PMSM). Dynamical equations of three time scale brushless DC motor system were presented by Ge and Cheng [10]. Chaotic anti-control and chaotic synchronization of the system were also studied. Fossi and Woafo [11] presented the dynamical model of an induction motor activating a mobile plate fixed to a spring and the electromechanical equations were formulated, and anti-control of chaos in the induction

motor was also obtained using the field-oriented control associated to the time delay feedback control. Anti-control of chaos in single time scale brushless DC motors (BLDCM) and chaotic synchronization of different order systems were also studied by Ge, Chang and Chen [12]. To control the undesirable chaos in the permanent magnet synchronous motor (PMSM), an adaptive dynamic surface control law was designed by Wei and his copartners [13]. The purpose of paper [14] was to employ time-delay feedback to anti-control a permanent magnet DC (PMDC) motor system for vibratory compactors. Yu et al. [15] developed an adaptive fuzzy control method to suppress chaos in the permanent magnet synchronous motor drive system via back stepping technology. However, there are few contributions to a current-driven induction motor, especially, the dynamical model for a whole induction motor system with indirect field controlled. While, it is a main drive device in modern industry, and its nonlinear vibration is catholic. Therefore, it is necessary to study the intrinsic quality of its nonlinear vibration via nonlinear dynamics theory.

Chaos control is inquisitive in how to control the chaotic system to the periodic orbit or equilibrium point with the original parameters remained or only fine-tuned, because the system parameters can not be changed objectively, or the parameters change largely must pay a great price. Typical control methods have been proposed to achieve chaos control. For instance, two methods of chaos control with a small time continuous perturbation were proposed by Pyragas [16]. Ataei et al. [17] presented a chaos synchronization method for a class of uncertain chaotic systems using the combination of an optimal control theory and an adaptive strategy. Wang and his coworkers [18] used symbolic dynamics and the automaton reset sequence to identify the current drive word and obtained the synchronization. Nonlinear and linear feedback controllers were designed to control and synchronize the chaotic system by Rafikov et al. [19]. Golovin et al. [20] proposed a global feedback control method based on measuring the maximum of the pattern amplitude over the domain, which can stabilize the system. Based on OGY approach, a multiparameter semi-continuous method was designed to control chaotic behavior by de Paula and Savi [21]. The united chaotic systems with uncertain parameters were synchronized based on the CLF method by Wang et al. [22]. Ataei et al. [23] presented a chaos synchronization method for a class of uncertain chaotic systems using the combination of an optimal control theory and an adaptive strategy. Among the control methods, sliding mode technique (SMT) is one of the best methods. Recently, many contributions have been published (see, for example, [24-28]). To our best knowledge, there is little information about control method, which could bridge the chaos control and synchronization from the literature. And, it is a very valuable theory for its stable and synchronous operation with the power system.

Considering all the above discussion, there are several advantages which make our approach attractive, compared with prior works. First, the nonlinear dynamical model for a whole induction motor system with indirect field controlled is proposed, and the nonlinear dynamics behaviors of the system model are analyzed including Poincare maps, bifurcation diagrams, dissipativity analysis and the spectrogram maps. Moreover, we present a sliding mode control method. And the control method is effective to the chaos control and synchronization. Numerical simulations are demonstrated to the effectiveness of the proposed scheme.

This paper is organized as follows. In Section 2, the nonlinear dynamical model of a current-driven induction motor expressed in a reference frame rotating at synchronous speed is proposed. Section 3 discusses the nonlinear dynamical behaviors of the system. In Section 4, a sliding mode controller is presented. Finally, we give the conclusions and discussions in Section 5.

2. **Problem Formulation and Preliminaries.** The nonlinear dynamical model of a current-driven induction motor expressed in a reference frame rotating at synchronous speed is given as follows:

$$\begin{cases} \dot{\phi}_{qr} = -\frac{R_r}{L_r}\phi_{qr} - \omega_{sl}\phi_{dr} + \frac{L_m}{L_r}R_r i_{qs} \\ \dot{\phi}_{dr} = -\frac{R_r}{L_r}\phi_{dr} - \omega_{sl}\phi_{qr} + \frac{L_m}{L_r}R_r i_{ds} \\ \dot{\omega}_r = -\frac{R_\omega}{J}\omega_r + \frac{1}{J}\left[\frac{3}{2}\frac{L_m}{L_r}n_p\left(i_{qs}\phi_{dr} - i_{ds}\phi_{qr}\right) - T_L\right] \end{cases} \tag{1}$$

where R_r is rotor resistance, L_r is rotor self-inductance, L_m is mutual inductance in a rotating reference frame, n_p is the number of pole pairs, ω_{sl} is slipping frequency, J is inertia coefficient, T_L is load, ϕ_{qr} is quadrature axis component, ϕ_{dr} is direct axis component of the rotor flux, ω_r is rotor angular speed and R_ω is rotating resistance coefficient, respectively.

The parameters are introduced as follows:

$$c_1 = \frac{R_r}{L_r}, \quad c_2 = \frac{L_m}{L_r}R_r, \quad c_3 = \frac{R_\omega}{J}, \quad c_4 = \frac{1}{J}, \quad c_5 = \frac{3}{2}\frac{L_m}{L_r}n_p,$$
$$x_1 = \phi_{qr}, \quad x_2 = \phi_{dr}, \quad u_1 = \omega_{sl}, \quad u_2 = i_{ds}, \quad u_3 = i_{qs}$$

Therefore, the nonlinear dynamical model of induction motor system with indirect field controlled can be rewritten as follows.

$$\begin{cases} \dot{x}_1 = -c_1 x_1 - u_1 x_2 + c_2 u_3 \\ \dot{x}_2 = -c_1 x_2 + u_1 x_1 + c_2 u_2 \\ \dot{\omega}_r = -c_3\omega_r + c_4\left[c_5\left(x_2 u_3 - x_1 u_2\right) - T_L\right] \end{cases} \tag{2}$$

In speed regulation applications, the indirect field oriented control is usually applied with a proportional integral (PI) speed loop, and this control strategy is described as follows:

$$\begin{cases} u_1 = \hat{c}_1 \frac{u_3}{u_2} \\ u_2 = u_2^0 \\ u_3 = K_p\left(\omega_{ref} - \omega_r\right) + K_i\int_0^t\left(\omega_{ref}(\zeta) - \omega_r(\zeta)\right)d\zeta \end{cases} \tag{3}$$

where $\hat{c}_1$ is the estimate for the inverse rotor time constant c_1, ω_{ref} is the constant reference velocity, u_2^0 is the constant reference for the rotor flux magnitude, K_p is the proportional of the PI speed regulator, K_i is the integral gains of the PI speed regulator.

The rotor time constant varies widely in practice IFOC system of IM. One sets $\hat{c}_1 = c_1$. That is to say, if it has a perfect estimate of the rotor time constant, the control is tuned; otherwise it is said to be detuned. Therefore, the degree of tuning is set to $k = \frac{\hat{c}_1}{c_1}$. Obviously, the controller is tuned and one sets $k = 1$.

Let $x_3 = \omega_{ref} - \omega_r$ and $x_4 = u_3$, and thus a new fourth dimensional system can be written as follows, based on the model of the whole closed-loop system (2) and the control strategy (3).

$$\begin{cases} \dot{x}_1 = -c_1 x_1 + c_2 x_4 - \frac{kc_1}{u_2^0}x_2 x_4 \\ \dot{x}_2 = -c_1 x_2 + c_2 u_2^0 + \frac{kc_1}{u_2^0}x_1 x_4 \\ \dot{x}_3 = -c_3 x_3 - c_4\left[c_5\left(x_2 x_4 - x_1 u_2^0\right) - T_L - \frac{c_3}{c_4}\omega_{ref}\right] \\ \dot{x}_4 = (k_i - k_p c_3)x_3 - k_p c_4\left[c_5\left(x_2 x_4 - x_1 u_2^0\right) - T_L - \frac{c_3}{c_4}\omega_{ref}\right] \end{cases} \tag{4}$$

3. **System Dynamics Analysis.** The phase trajectory is most intuitive way to describe system state, shown in Figure 1, when $c_1 = 13.67$, $c_2 = 1.56$, $c_3 = 0.59$, $c_4 = 1176$, $c_5 = 2.86$, $u_2^0 = 4$, $k_p = 0.001$, $k_i = 1$, $k = 1.5$, $T_L = 0.5$, $\omega_{ref} = 181.1$ and the initial state is set $x_1 = 0$, $x_2 = 0.4$, $x_3 = -200$, $x_4 = 6$.

Poincare map is a classic technology of dynamical system analysis. If the dense point on the Poincare section is flaky and structural, the system is chaotic. The Poincare map is got in the plane $z = 1.5$, shown in Figure 2. Meanwhile, the spectrogram map exhibits continuous broadband feature, shown in Figure 3.

(a) x_1-x_2-x_3

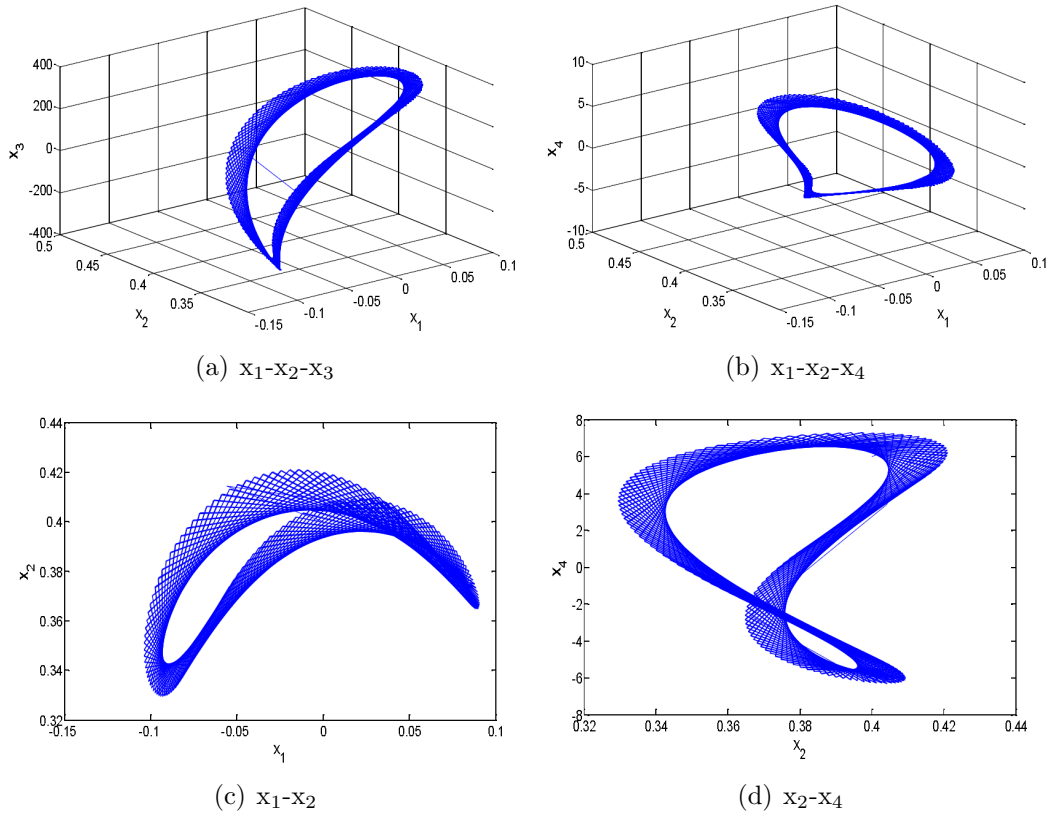(b) x_1-x_2-x_4

(c) x_1-x_2

(d) x_2-x_4

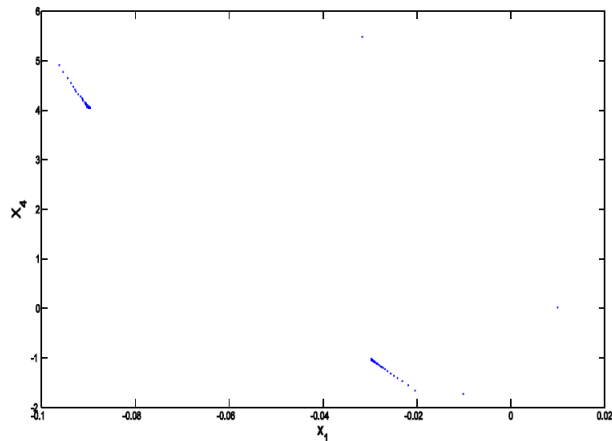FIGURE 1. Phase trajectory for system (4)
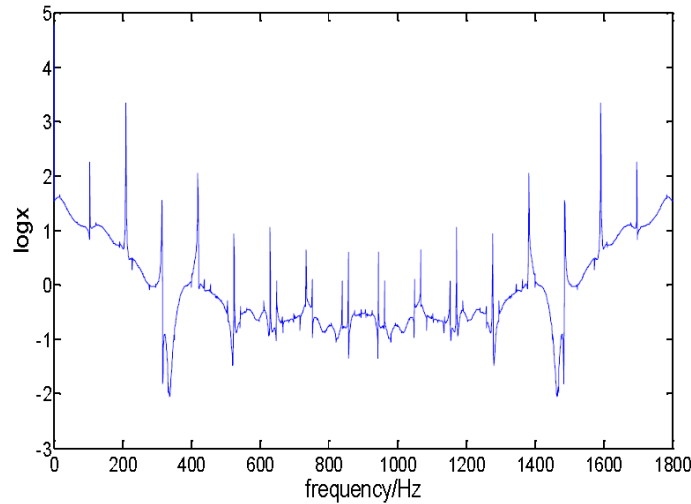

FIGURE 2. Poincare map for system (4)
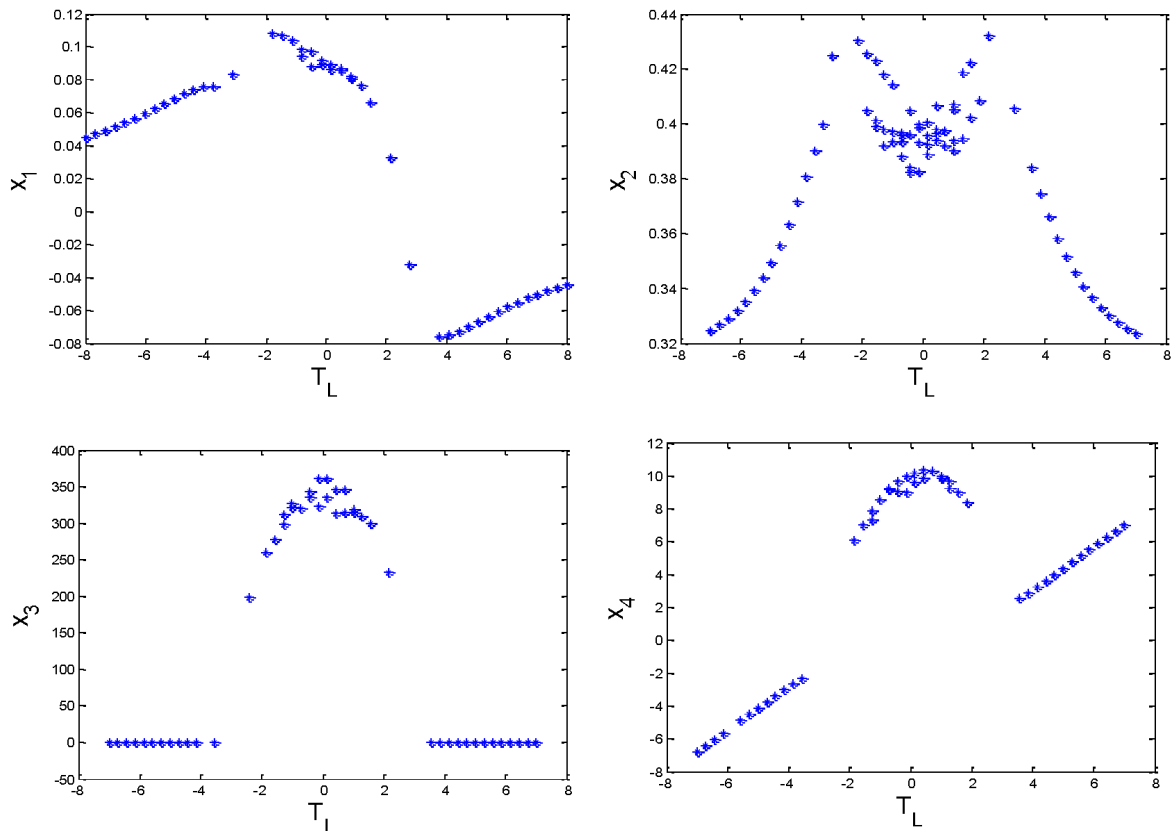
FIGURE 3. Spectrogram for system (4)

FIGURE 4. Hopf bifurcation with the change of T_L for system (4)

A bifurcation diagram summarizes the essential dynamics of a system, and thus is a useful tool to observe its nonlinear dynamical response. The bifurcation diagram is shown in Figure 4 with different torque TL parameters for system (4). The parameters of the motor are listed as $c_1 = 13.67s^{-1}$, $c_2 = 1.56H \cdot s^{-1}$, $c_3 = 0.59s^{-1}$, $c_4 = 1176kg^{-1} \cdot m^{-2}$ and $c_5 = 2.86$, the parameters of the system are given $u_2^0 = 4A$, $\omega_{ref} = 181.1rad/s$, $k_p = 0.001$, $k_i = 0.5$, and $k = 1.5$.

The equilibria of system (4) can be found by solving the following algebraic equations:

$$\begin{cases} 0 = -c_1 x_1 + c_2 x_4 - \frac{kc_1}{u_2^0} x_2 x_4 \\ 0 = -c_1 x_2 + c_2 u_2^0 + \frac{kc_1}{u_2^0} x_1 x_4 \\ 0 = -c_3 x_3 - c_4 \left[c_5 \left(x_2 x_4 - x_1 u_2^0 \right) - T_L - \frac{c_3}{c_4} \omega_{ref} \right] \\ 0 = (k_i - k_p c_3) x_3 - k_p c_4 \left[c_5 \left(x_2 x_4 - x_1 u_2^0 \right) - T_L - \frac{c_3}{c_4} \omega_{ref} \right] \end{cases}$$

where, $c_1 = 13.67$, $c_2 = 1.56$, $c_3 = 0.59$, $c_4 = 1176$, $c_5 = 2.86$, $u_2^0 = 4$, $k_p = 0.001$, $k_i = 1$, $k = 1.5$, $T_L = 0.5$, $\omega_{ref} = 181.1$ and the initial state is set to $x_1 = 0$, $x_2 = 0.4$, $x_3 = -200$, $x_4 = 6$.

The system has three equilibria, which are respectively described as follows:
O$(-0.017, 0.455, 0, 0.304)$,
E$^+(-0.022 - 0.182 * i, 0.184 + 0.021 * i, 0, 0.187 - 3.981 * i)$,
E$^-(-0.022 + 0.182 * i, 0.184 - 0.021 * i, 0, 0.187 + 3.981 * i)$.

The system has a unique equilibrium O$(-0.017, 0.455, 0, 0.304)$. Linearize the system at O, and the Jacobian matrix is obtained as follows:

$$J_0 = \begin{bmatrix} -13.67 & -5.12625 x_4 & 0 & 1.56 - 5.12625 x_2 \\ 5.12625 x_4 & -13.67 & 0 & 5.12625 x_1 \\ 13453.44 & -3363.36 x_4 & -0.59 & -3363.36 x_2 \\ 13.45344 & -3.36336 x_4 & 0.99941 & -3.36336 x_2 \end{bmatrix}$$

$$= \begin{bmatrix} -13.67 & -1.558 & 0 & -0.772 \\ 1.558 & -13.67 & 0 & -0.087 \\ 13453.44 & -1022.46 & -0.59 & -1530.32 \\ 13.4534 & -1.022 & 0.999 & -1.530 \end{bmatrix}$$

For gaining its eigenvalues, we have:

$$|\lambda I - J_0| = 0$$

These eigenvalues at equilibrium O are respectively obtained as follows:

$$\lambda_1 = 1.65 + 40.39i, \quad \lambda_2 = 1.65 - 40.39i, \quad \lambda_3 = -18.98, \quad \lambda_4 = -13.78.$$

λ_1, λ_2 are complex conjugate pair and their real parts are positive, and λ_3 and λ_4 are negative real numbers. Therefore, the equilibrium O is a saddle point. It is unstable.

The other two equilibrium points E$^+$ and E$^-$ do not belong to the real space. Thus, it is not necessary to discuss stability of these points.

The theory of dissipative systems is a basic tool to describe the system characteristics. And dissipative analysis of system (4) is presented as follows. For system (4), it is noticed that

$$\nabla V = \frac{\partial \dot{x}_1}{\partial x_1} + \frac{\partial \dot{x}_2}{\partial x_2} + \frac{\partial \dot{x}_3}{\partial x_3} + \frac{\partial \dot{x}_4}{\partial x_4} = - \left(2c_1 + c_3 + k_p c_4 c_5 x_2 \right) < 0,$$

where $c_1 = 13.67$, $c_3 = 0.59$, $c_4 = 1176$, $c_5 = 2.86$, $k_p = 0.001$ and $0.32 \leq x_2 \leq 0.42$. Obviously, system (4) can have dissipative structure, with an exponential contraction rate:

$$\frac{dV}{dt} = - \left(2c_1 + c_3 + k_p c_4 c_5 x_2 \right) V.$$

That is, a volume element V_0 is contracted by the flow into a volume element $V_0 e^{-(2c_1 + c_3 + k_p c_4 c_5 x_2)t}$ in time t. This means that each volume containing the system orbit shrinks to zero as $t \to \infty$ at an exponential rate $-\left(2c_1 + c_3 + k_p c_4 c_5 x_2 \right)$. Therefore, all

system orbits are ultimately confined to some subset of zero volume, and the asymptotic motion settles on some attractors.

4. Chaos Control, Synchronization and Numerical Simulation Results.

4.1. Controller design. Consider the drive system

$$Dx = Ax + g(x) \tag{5}$$

where $x(t) \in R^4$ denotes the state vector of the 4-dimensional system, $A \in R^{4 \times 4}$ represents the linear part of the system and $g : R^4 \to R^4$ is the nonlinear part of the system.

Considering $y(t) \in R^4$ as the response of state vector of the 4-dimensional system, we can rewrite the response system as

$$Dy = Ay + g(y) \tag{6}$$

The controller $u(t) \in R^4$ is added to system (6), so it can be rewritten as:

$$Dy = Ay + g(y) + u(t) \tag{7}$$

Here, we define the synchronization errors $e = y - x$. The aim is to choose a suitable controller $u(t) \in R^4$ such that the states of the master and slave systems can reach synchronization (i.e., $\lim_{t \to \infty} \|e\| = 0$, where $\|\cdot\|$ is the Euclidean norm).

Now, one sets the controller $u(t)$ as

$$u(t) = u_1(t) + u_2(t) \tag{8}$$

where $u_1(t) \in R^4$ is a compensation controller, and $u_1(t) = Dx - A(x) - g(x)$. $u_2(t) \in R^4$ is a vector function, and will be designed later. Using (8), response system (7) can be rewritten as

$$De(t) = Ae + g(y) - g(x) + u_2(t) \tag{9}$$

In accordance with the procedure of designing active controller, the nonlinear part of the error dynamics is eliminated by the following the following input vector:

$$u_2(t) = g(x) - g(y) + Kw(t) \tag{10}$$

Error system (9) is then rewritten as follows

$$De(t) = Ae + Kw(t) \tag{11}$$

where $K = [k_1, k_2, k_3, k_4]^{\mathrm{T}}$ is a constant gain vector and $w(t) \in R$ is the control input that satisfies

$$w(t) = \begin{cases} w^+(t) & s(e) \geq 0 \\ w^-(t) & s(e) < 0 \end{cases} \tag{12}$$

As a choice for the sliding surface, we have

$$s(t) = Ce \tag{13}$$

where $C = [c_1, c_2, c_3, c_4]^{\mathrm{T}}$ is a constant vector. For sliding mode method, the sliding surface and its derivative must satisfy the following conditions.

$$s(t) = 0, \quad \dot{s}(t) = 0 \tag{14}$$

One sets:

$$\dot{s}(t) = CDe(t) = C(Ae + Kw(t)) = 0 \tag{15}$$

To satisfy the above condition, the discontinuous reaching law is chosen as follows

$$Ds(t) = -psign(s) - rs \tag{16}$$

where

$$sign(s) = \begin{cases} +1, s > 0 \\ 0, s = 0 \\ -1, s < 0 \end{cases} \tag{17}$$

and $p > 0$, $r > 0$ are the gains of the controller.

Considering (15) and (16), we have

$$w(t) = -(CK)^{-1}\left[C(rI + A)e + psign(s)\right] \tag{18}$$

Now, the total control law can be defined as follows

$$u(t) = Dx - Ax - g(y) - K(CK)^{-1}\left[C(rI + A)e + psign(s)\right] \tag{19}$$

Using (19) and (9), the error dynamics can be obtained

$$De = [A - K(CK)^{-1}C(rI + A)]e - K(CK)^{-1}psign(s) \tag{20}$$

For the sliding term, a linear system is a bounded input ($-K(CK)^{-1}p$, when $s > 0$ and $K(CK)^{-1}p$, when $s < 0$). The system (20) is stable, if $|\arg(eig([A - K(CK)^{-1}C(rI + A)]))| > \pi/2$. It can be shown that choosing appropriate K, C and r can make the error dynamics stable. Hence, the synchronization is realized.

Similarly, if the drive system (5) is modified as

$$Dx = 0 \tag{21}$$

Thus, the response system can be controlled to the initial values of drive system. If the initial values are changed, the controlling to any stable point can be achieved.

4.2. **Numerical simulation results.** The numerical simulation results are carried out to verify the applicability and effectiveness of the proposed sliding mode control method. It should be noticed that the controller is in action at $t = 10$. The ode45 solver of Matlab software is applied to solve different equations. By taking the parameters as these in Section 3, system (4) can be rewritten as:

$$\begin{cases} \dot{x}_1 = -13.67x_1 + 1.56x_4 - 5.1262x_2x_4 \\ \dot{x}_2 = -13.67x_2 + 5.1262x_1x_4 + 6.24 \\ \dot{x}_3 = -0.59x_3 - 3363.4x_2x_4 + 13453x_1 + 694.85 \\ \dot{x}_4 = 0.9994x_3 - 3.3634x_2x_4 + 13.4534x_1 + 0.6948 \end{cases} \tag{22}$$

According to 4.1, we get

$$A = \begin{bmatrix} -13.67 & 0 & 0 & 1.56 \\ 0 & -13.67 & 0 & 0 \\ 13453 & 0 & -0.59 & 0 \\ 13.4534 & 0 & 0.9994 & 0 \end{bmatrix}, \quad g = \begin{bmatrix} -5.1262x_2x_4 \\ 5.1262x_1x_4 + 6.24 \\ -3363.4x_2x_4 + 694.85 \\ -3.3634x_2x_4 + 0.6948 \end{bmatrix}$$

Let system (22) with initial conditions $[x_{d1}, x_{d2}, x_{d3}, x_{d4}]^T = [0, 0.4, -200, 6]^T$ as a drive system, and system (22) with initial values $[x_{r1}, x_{r2}, x_{r3}, x_{r4}]^T = [0.3, 0.5, 0.2, 0.4]^T$ as a response system. The parameters of the controller are set as $K = [-2, -6, -2, -2]^T$, $C = [5, 5, 5, 5]$, $r = 5$, and $p = 0.2$. This selection of parameters results in eigenvalues $(\lambda_1, \lambda_2, \lambda_3, \lambda_4) = (-2247.3, -14.072, -5, -2.1495)$ which are located in the stable region.

According to (19), the control signals are obtained as

$$
\begin{cases}
u_1 = \frac{d^{q_{r1}}x_d}{dt} - 2243.0e_1 + 1.4450e_2 - 0.9016e_3 - 1.0933e_4 \\
\qquad + 13.670x_d - 1.56w_d + 5.1262y_rw_r - 0.0067sign(s_1) \\
u_2 = \frac{d^{q_{r2}}y_d}{dt} - 6728.9e_1 + 4.3350e_2 - 2.7047e_3 - 3.28e_4 \\
\qquad + 13.67y_d - 5.1262x_rw_r - 6.24 - 0.02sign(s_2) \\
u_3 = \frac{d^{q_{r3}}z_d}{dt} - 2243.0e_1 + 1.4450e_2 - 0.90157e_3 - 1.0933e_4 \\
\qquad - 13453x_d + 0.59z_d + 3363.4y_rw_r - 694.85 - 0.0067sign(s_3) \\
u_4 = \frac{d^{q_{r4}}w_d}{dt} - 2243.0e_1 + 1.4450e_2 - 0.90157e_3 - 1.0933e_4 \\
\qquad - 13.453x_d - 0.9994z_d + 3.3634y_rw_r - 0.6948 - 0.0067sign(s_4)
\end{cases}
\tag{23}
$$

where $e_1 = x_r - x_d$, $e_2 = y_r - y_d$, $e_3 = z_r - z_d$, $e_4 = w_r - w_d$.

The numerical simulation results are given in Figure 5. One can see, the errors converge to zero immediately after the controller was applied, which implies that the chaos synchronization between the two systems is realized.

Keep the parameters of the controller fixed, while set the drive system as system (21) to investigate the effectiveness of the controller. And we still use system (23) as the controller. Fortunately, Figure 6 illustrates the response states, which show that the response states follow initial values of the drive system immediately.

5. **Conclusions and Discussions.** The drive system of induction motor with indirect field controlled is studied in this paper. The system model is described, which is an autonomous four-order electromechanical system. In order to analyze a variety of chaotic
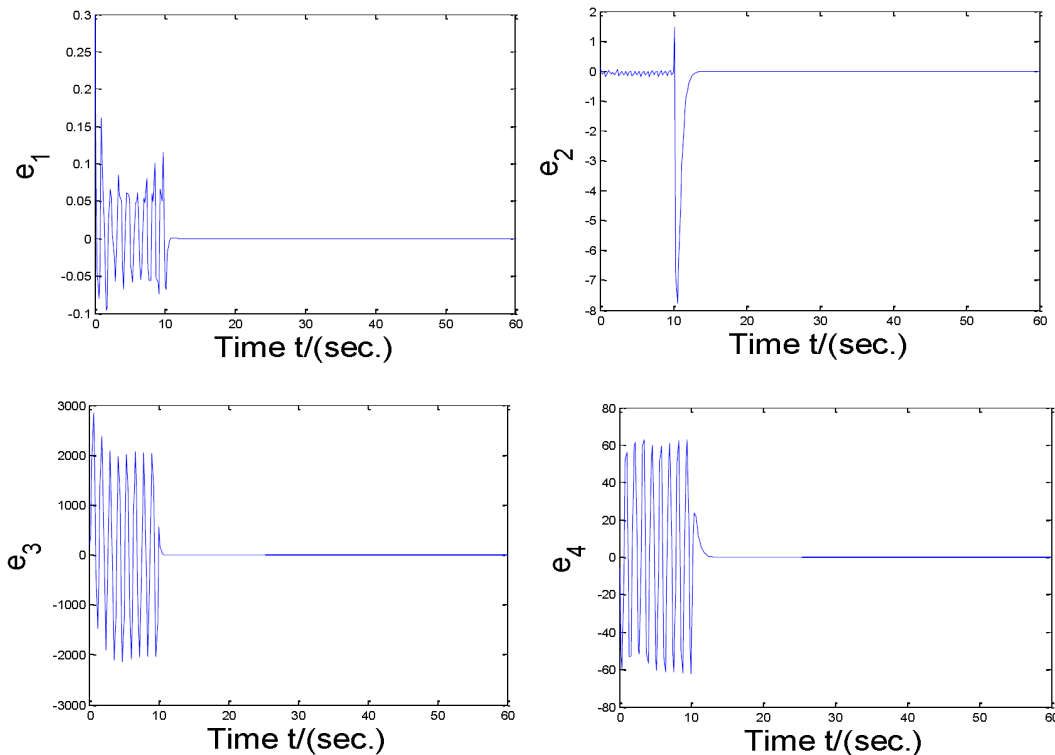

FIGURE 5. Synchronization errors between the two systems (the controller $u(t)$ is activated at $t = 10$)
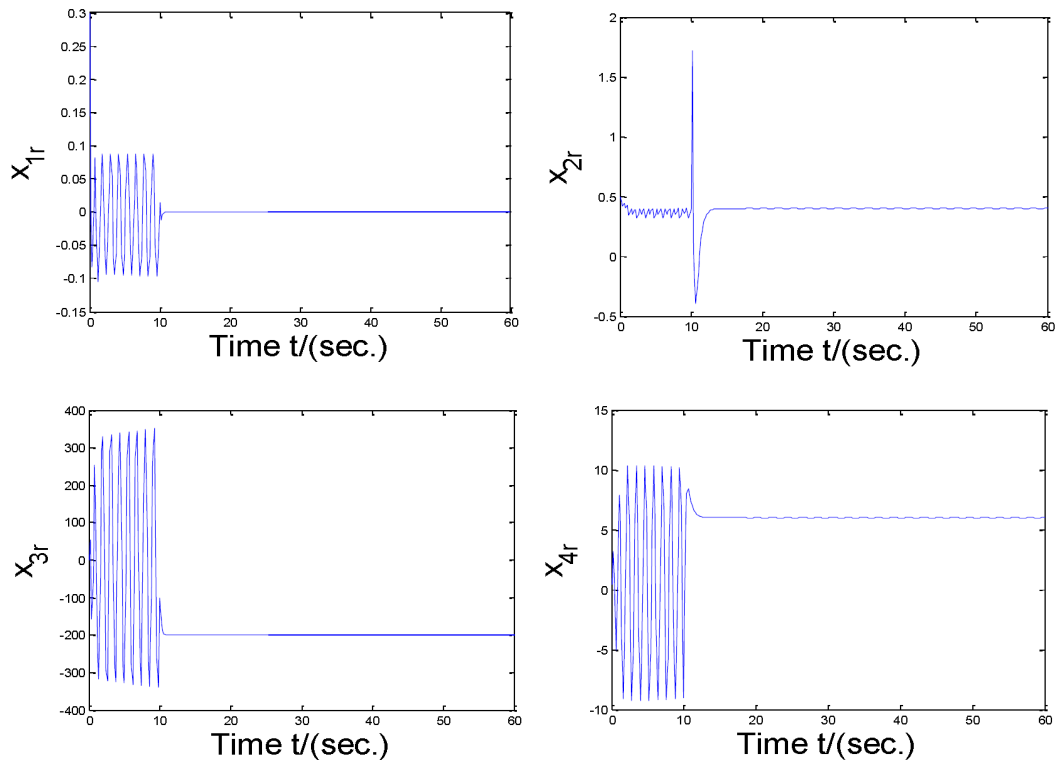
FIGURE 6. The state variables of the response system in the presence of controller (the controller $u(t)$ is activated at $t = 10$)

phenomena, we employ several numerical techniques such as phase portrait, bifurcation diagrams, Poincare map, balance point, Spectrogram map and dissipativity. To understand the complex dynamics of system, some basic dynamical properties, such as equilibrium, stability are rigorously derived and studied. Chaotic attractors are first numerically verified through investigating phase trajectories, bifurcation path and Poincaré projections and dissipativity. All of the above is theoretical basis of stability of an induction motor system with indirect field controlled.

Synchronization and control of the chaos in the induction motor system based on sliding mode law is proposed. The theoretical analysis and numerical results have shown the effectiveness of the proposed controller. Moreover, the sliding mode law is a bridge between chaos control and synchronization, which provides a theoretical support for its stable and synchronous operation with the power system.

In fact, the electrical devices are all nonlinear system. With the rapid development of nonlinear science, it comes true that many nonlinear models can be described and analyzed. Furthermore, the more and better control methods for different situations should be studied. For example, new controller is with fewer terms, new control method has better immunity against noise and uncertain parameters.

REFERENCES

[1] D. Y. Chen, Y. X. Liu, X. Y. Ma and R. F. Zhang, Control of a class of fractional-order chaotic systems via sliding mode, *Nonlinear Dynamics*, vol.67, no.1, pp.893-901, 2012.

[2] J. Zhang, C. S. Zhou, X. K. Xu and M. Small, Mapping from structure to dynamics: A unified view of dynamical processes on networks, *Physical Review E*, vol.82, no.2, pp.026116, 2010.

[3] D. Y. Chen, W. L. Zhao, X. Y. Ma et al., No-chattering sliding mode control chaos in Hindmarsh-Rose neurons with uncertain parameters, *Computers and Mathematics with Applications*, vol.61, no.8, pp.3161-3171, 2011.

[4] C. A. Kitio Kwuimy, B. Nana and P. Woafo, Experimental bifurcations and chaos in a modified self-sustained macro electromechanical system, *Journal of Sound and Vibration*, vol.329, no.15, pp.3137-3148, 2010.

[5] D. Y. Chen, C. Wu, C. F. Liu et al., Synchronization and circuit simulation of a new double-wing chaos, *Nonlinear Dynamics*, vol.67, no.2, pp.1481-1504, 2012.

[6] M. Ataei, A. Kiyoumarsi and B. Ghorbani, Control of chaos in permanent magnet synchronous motor by using optimal Lyapunov exponents placement, *Physics Letters A*, vol.374, no.41, pp.4226-4230, 2010.

[7] Z. J. Jing, C. Yu and G. R. Chen, Complex dynamics in a permanent-magnet synchronous motor model, *Chaos, Solitons and Fractals*, vol.22, no.4, pp.831-848, 2004.

[8] A. M. Harb and A. A. Zaher, Nonlinear control of permanent magnet stepper motors, *Communications in Nonlinear Science and Numerical Simulations*, vol.9, no.4, pp.443-458, 2004.

[9] M. Zribi, A. Oteafy and N. Smaoui, Controlling chaos in the permanent magnet synchronous motor, *Chaos, Solitons and Fractals*, vol.41, no.3, pp.1266-1276, 2009.

[10] Z. M. Ge and J. W. Cheng, Chaos synchronization and parameter identification of three time scales brushless DC motor system, *Chaos, Solitons and Fractals*, vol.24, no.2, pp.597-616, 2005.

[11] D. O. T. Fossi and P. Woafo, Dynamical behaviors of a plate activated by an induction motor, *Journal of Sound and Vibration*, vol.329, no.17, pp.3507-3519, 2010.

[12] Z. M. Ge, C. M. Chang and Y. S. Chen, Anti-control of chaos of single time scale brushless DC motors and chaos synchronization of different order system, *Chaos, Solitons and Fractals*, vol.27, no.5, pp.1298-1315, 2006.

[13] D. Q. Wei, X. S. Luo, B. H. Wang et al., Robust adaptive dynamic surface control of chaos in permanent magnet synchronous motor, *Physics Letters A*, vol.363, no.1-2, pp.71-77, 2007.

[14] Z. Wang and K. T. Chau, Anti-control of chaos of a permanent magnet DC motor system for vibratory compactors, *Chaos, Solitons and Fractals*, vol.36, no.3, pp.694-708, 2008.

[15] J. P. Yu, B. Chen, H. S. Yu et al., Adaptive fuzzy tracking control for the chaotic permanent magnet synchronous motor drive system via backstepping, *Nonlinear Analysis: Real World Applications*, vol.12, no.1, pp.671-681, 2011.

[16] K. Pyragas, Continuous control of chaos by self-controlling feedback, *Physics Letters A*, vol.170, no.6, pp.421-428, 1992.

[17] M. Ataei, A. Iromloozadeh and B. Karimi, Robust synchronization of a class of uncertain chaotic systems based on quadratic optimal theory and adaptive strategy, *Chaos*, vol.20, no.4, pp.043137, 2010.

[18] M. G. Wang, X. Y. Wang, Z. Z. Liu and H. G. Zhang, The least channel capacity for chaos synchronization, *Chaos*, vol.21, no.1, pp.013107, 2011.

[19] M. Rafikov and J. M. Balthazar, On control and synchronization in chaotic and hyperchaotic systems via linear feedback control, *Communications in Nonlinear Science and Numerical Simulation*, vol.13, no.7, pp.1246-1255, 2008.

[20] A. A. Golovin, Y. Kanevsky and A. A. Nepomnyashchy, Feedback control of subcritical Turing instability with zero mode, *Physical Reiview E*, vol.79, no.4, pp.046218, 2009.

[21] A. S. de Paula and M. A. Savi, A multiparameter chaos control method based on OGY approach, *Chaos, Solitons & Fractals*, vol.40, no.3, pp.1376-1390, 2009.

[22] H. Wang, Z. Z. Han, W. Zhang and Q. Y. Xie, Synchronization of united chaotic systems with uncertain parameters based on the CLF, *Nonlinear Analysis: Real World Applications*, vol.10, no.2, pp.715-722, 2009.

[23] M. Ataei, A. Iromloozadeh and B. Karimi, Robust synchronization of a class of uncertain chaotic systems based on quadratic optimal theory and adaptive strategy, *Chaos*, vol.20, no.4, pp.043137, 2010.

[24] P. Shi, Y. Xia, G. Liu and D. Rees, On designing of sliding mode control for stochastic jump systems, *IEEE Trans. on Automatic Control*, vol.51, no.1, pp.97-103, 2006.

[25] D. Y. Chen, T. Shen and X. Y. Ma, Sliding mode control of chaotic vibrations of spinning disks with uncertain parameter under bounded disturbance, *Acta Physica Sinica*, vol.60, no.5, pp.050505, 2011 (in Chinese).

[26] D. Y. Chen, Y. X. Liu, X. Y. Ma et al., No-chattering sliding mode control in a class of fractional-order chaotic systems, *Chinese Phyiscs B*, vol.20, no.12, pp.120506, 2011.

[27] B. Jiang, P. Shi and Z. Mao, Sliding mode observer-based fault estimation for nonlinear networked control systems, *Circuits Systems and Signal Processing*, vol.30, no.1, pp.1-16, 2011.

[28] D. Y. Chen, R. F. Zhang, X. Y. Ma et al., Chaotic synchronization and anti-synchronization for a novel class of multiple chaotic systems via a sliding mode control scheme, *Nonlinear Dynamics*, vol.69, no.1-2, pp.35-55, 2012.